Original Article

Modification of erythrocytes by internalizing Arg-Gly-Asp (iRGD) in boosting the curative effect of radiotherapy for gastric carcinoma

Chong Zhou, Qin Liu, Fanyan Meng, Naiqing Ding, Jing Yan, Baorui Liu

The Comprehensive Cancer Centre of Nanjing Drum Tower Hospital, Clinical College of Nanjing Medical University, Nanjing, China

Contributions: (I) Conception and design: B Liu, Q Liu; (II) Administrative support: B Liu; (III) Provision of study materials or patients: J Yan, F Meng; (IV) Collection and assembly of data: C Zhou; (V) Data analysis and interpretation: C Zhou, N Ding; (VI) Manuscript writing: All authors; (VII) Final approval of manuscript: All authors.

Correspondence to: Baorui Liu. The Comprehensive Cancer Centre of Nanjing Drum Tower Hospital, Clinical College of Nanjing Medical University, 321 Zhongshan Road, Nanjing 210000, China. Email: baoruiliu@nju.edu.cn.

Background: Radiation resistance remains the leading cause of radiotherapy (RT) failure. The development of tumor-specific targeted sensitizers is key to overcoming radiation resistance. Our early data showed that cancer cell penetration was simulated by internalizing arginine-glycine-aspartic acid (iRGD), and the irradiation efficacy was improved. The present study aims to design and fabricate iRGD-modified red blood cell (RBCs) for tumor targeting and RT enhancement, and to evaluate its safety and efficacy *in vivo*.

Methods: 1,2-Distearoyl-sn-glycero-3-phosphoethanolamine-poly ethylene glycol-iRGD (DSPE-PEG-iRGD) was used to modify RBCs by a lipid-insertion method without direct chemical bioconjugation. Fluorescent dyes were used to trace the functional RBCs through confocal microscopy examination. *In vitro* stability evaluation was performed using cell culture medium incubation for 48 h followed by fluorescence decay assay. Furthermore, a subcutaneous cancer cell mouse model was constructed with MKN-45 cells for target efficacy and RT enhancement evaluation with DSPE-PEG-iRGD-modified RBCs (RBC-iRGD).

Results: Successful construction of RBC-iRGD was verified by the presence of the yellow fluorescence, and an approximately 10^8 iRGD molecules were labeled on a single RBC. The final RBC-iRGD showed good stability without any hemolytic effects in the cell culture medium. Moreover, higher fluorescence intensity and decreased liver and spleen accumulation could be observed in RBC-iRGD compared to RBC + iRGD *in vivo*. The RBC-iRGD exerted enhanced radiosensitivity in subcutaneous gastric tumor mice.

Conclusions: The RBC-iRGD exerted good tumor-targeting efficacy and favorable effects for RT enhancement *in vivo*.

Keywords: Internalizing arginine-glycine-aspartic acid (iRGD); erythrocytes; gastric cancer (GC); tumor targeting; radiotherapy (RT)

Submitted Sep 19, 2022. Accepted for publication Oct 18, 2022.
doi: 10.21037/jgo-22-951
View this article at: https://dx.doi.org/10.21037/jgo-22-951

Introduction

Gastric cancer (GC) is a kind of tumor with high mortality and incidence reported across Eastern and Western Asia (1). The treatment of locally advanced and/or metastatic GC remains a challenge despite recent advancements in therapeutic modalities and chemotherapy agents (2). An increasing amount of evidence has demonstrated that radiotherapy (RT) as a local treatment modality can exert a good therapeutic effect (3-5). However, tumor resistance to irradiation, as well as acute and late toxicity resulting from RT, has limited its efficacy in clinical cancer treatment (6,7). Therefore, there is an urgent need to formulate novel and practical strategies to overcome tumor resistance to RT and reduce its toxicity on the normal tissues and organs surrounding the tumor.

It is well known that the effects of RT are affected by hypoxia. To enhance tumor radiosensitivity, a variety of strategies have been developed to alleviate tumor hypoxia, and the most direct and effective way is to improve oxygen supply in the hypoxic area. Different methods have been developed to transport oxygen to cancer cells, including employing liquids with high oxygen solubility, administering hemoglobin, and introducing oxygen-generating agents, among others (8-10).

Erythrocytes or red blood cell (RBCs), as natural oxygen carriers, have several advantages that make them suitable as radiosensitizers. RBCs are abundant, biocompatible, affordable, and easy to isolate. In addition, RBCs can circulate in humans for about 3 months and in mice for about 40 days. The prevailing belief is that internalizing arginine-glycine-aspartic acid (iRGD) could work as a "deliveryman" for peptide-mediated transport of compounds deep into the tissue parenchyma (11). In one study, iRGD-conjugated compounds were injected intravenously (IV) to bind to tumor vessels and infiltrate into extravascular tumor parenchyma (12). Some studies reported iRGD to deliver drugs deep into tumor tissues in gastric cancer (13,14). Recently, iRGD has entered phase one clinical trials and has shown good safety (15). The research interests of our laboratory is to use the tumor-penetrating peptide iRGD to improve the efficacy of anti-tumor therapy. Our previous study reported for the first time that the modification of iRGD could improve the cancer-specific lymphocyte infiltration in both mouse models and 3D cancer spheroids (16). Recently, we demonstrated that iRGD could enhance irradiation efficacy via remodeling tumor tissue penetration (17). However, the feasibility of employment of iRGD for RBC modification has not been reported yet. There are several surface attachment techniques that can modify membranes of RBCs to improve the active tumor-targeting ability of RBCs. Fang *et al.* employed a lipid-insertion technique to functionalize both folate and the nucleoli-targeting aptamer AS1411 to allow RBCs to obtain receptor-specific targeting against model cancer cell lines (18), which has provided us additional insight into RBC modification. We subsequently designed and fabricated RBC-iRGD for tumor targeting and therapy enhancement, evaluated their safety and efficacy *in vivo*, and investigated the possible mechanisms involved in its effects using an *in vitro* cell system. The results demonstrated that RBC-iRGD exert good tumor-targeting efficacy and provide favorable effects for RT enhancement *in vivo*. We present the following article in accordance with the ARRIVE reporting checklist (available at https://jgo.amegroups.com/article/view/10.21037/jgo-22-951/rc).

Methods

Reagents

Tumor-penetration peptide iRGD (cyclic CRGDKGPDC), Cys-iRGD (Cys-CRGDKGPDC), and Fam-CCRGDKGPDC-NH2 were custom-synthesized by ChinaPeptides Co., Ltd. (Shanghai, China).

Cell line

Human GC cell line MKN-45 was obtained from the Chinese Academy of Sciences Cells Bank (Shanghai, China). Cells were cultured in RPMI 1640 medium (Wisent, Nanjing, China).

Mice

Seven-week-old male BALB/c athymic nude mice were provided by Yangzhou University. Experiments were performed under a project license (No. 20150902) granted by the Animal Care Committee at Nanjing Drum Tower Hospital, in compliance with Nanjing Drum Tower Hospital guidelines for the care and use of animals. A protocol was prepared before the study without registration.

Synthesis of 1,2-distearoyl-sn-glycero-3-phosphoethanolamine-poly ethylene glycol-iRGD (DSPE-PEG-iRGD)

DSPE-PEG-MAL was mixed with C-iRGD at a 1:1 molar ratio in HEPES buffer (pH =6.5). The reaction mixture was incubated for 48 h at room temperature (RT) in a shaker, and the resulting reaction mixture was placed in a dialysis bag (molecular weight cutoff =3,500 Da) and dialyzed in double-distilled water for 48 h to remove small molecules. The final solution in the dialysis bag was lyophilized and stored at –20 ℃ until used.

Modification of RBCs with DSPE-PEG-iRGD

Whole blood was collected from the anaesthetized mice into heparin sodium salt tubes via cardiac puncture. RBCs were extracted from blood by centrifugation at 1,200 ×g for 5 min at 4 ℃ and washed 3 times in phosphate-buffered

saline (PBS). The washed RBCs were resuspended in PBS to a final RBC concentration of 5×10^8/mL, and then incubated with various amounts of DSPE-PEG-iRGD at RT for 30 min to form iRGD-inserted RBCs (RBC-iRGD), following the methodology reported by Shi *et al.* (19). The inserted RBCs were then washed 3 times with PBS before further use.

Characterization of RBC-iRGD

RBC-iRGD were examined with confocal microscopy for the emission of the yellow color, and the conjugation efficacy of iRGD and RBCs was calculated by a linear regression equation using the parameters of fluorescence intensity and iRGD concentration.

In vitro stability evaluation of RBC-iRGD

RBCs alone, RBC + iRGD, or RBC-iRGD were incubated in RPMI 1640 medium containing 10% fetal bovine serum (FBS) for 48 h. Fluorescence decay was evaluated by confocal microscopy examination. Moreover, hemolytic RBCs prepared by 0.5-time PBS incubation for 5 min were used as control for hemolytic effects evaluation.

In vivo near-infrared fluorescence imaging and in vivo immunofluorescence

A subcutaneous xenograft model was established by injecting 10^6 MKN-45 cells in 100 µL of PBS subcutaneously in male Balb/c nude mice. The PBS-washed RBC suspension with or without iRGD modification (5×10^8/mL in PBS, 500 µL) was incubated with the same volume of DiR solution (10 µM in DBPS diluted from 2 mM DiR in ethanol) for 30 min at room temperature under 100 rpm. The DiR-stained RBCs were used for monitoring the *in vivo* biodistribution of the RBCs.

Once the tumor volume in the xenografts reached ~300 mm^3, 200 µL of DiR-prestained RBCs, DiR-prestained RBCs coadministrated with free iRGD or DiR-prestained RBC-iRGD was IV administrated via the tail vein of the tumor-bearing nude mice. Each mouse was treated with 10^8 RBCs. Anesthesia was maintained with inhaled isoflurane [1.0–2.5% (vol/vol)] for the duration of the experiment. Animal temperature was maintained at 37 ℃ using a heating plate and scanned using a Maestr Automated In Vivo Imaging System (Cambridge Research & Instrumentation Inc., Woburn, MA, USA).

In vivo irradiation enhancement efficacy and safety assay

For IR treatment, Balb/c nude mice bearing MKN-45 tumors were prepared. The mice were randomized and assigned into 6 groups (n=5/group): 1, control (PBS injection); 2, RBC + iRGD; 3, RBC-iRGD; 4, irradiation (IR); 5, IR + RBC + iRGD; and 6, IR + RBC-iRGD. Mice in group 4, 5, and 6 received an irradiation with 3 fractions of 5 Gy a day. Irradiations were performed 10 days after the tumor was inoculated using linear generator. Administration of RBCs at 10^8 cells per mouse, RBC (exact quantities as above) + iRGD (1 mg per mouse), or RBC-iRGD (same quantities as above) commenced at the time of 6 hours before fractionated IR via IV injection.

On day 21 after IV injection, 1 mouse from each group was randomly selected and killed. The main organs (heart, liver, spleen, lungs, and kidneys) were dissected; fixed in 10% neutral-buffered formalin, embedded in paraffin, sliced into 10-µm-thick sections; sectioned and stained with hematoxylin and eosin, and then examined under optical microscopy.

Statistical analysis

All statistical analyses and experimental charts were performed using GraphPad Prism 6 (GraphPad Inc., San Diego, CA, USA). All values provided represent mean ± standard deviation unless otherwise noted. Normally distributed data were evaluated with analysis of variance (ANOVA). Statistical significance was set as follows: $P<0.05$.

Results

Fabrication of iRGD modified RBCs

RBC-iRGD were designed according to the procedure outlined in *Figure 1*. We successfully synthesized DSPE-PEG-iRGD and analyzed it by matrix-assisted laser desorption/ionization time-of-flight mass spectrometry (MALDI-TOF MS) (16). In our experiments, RBC-iRGD were generated by modification of DiI-stained (DiI is a cell membrane fluorescently labeled dye that emits red fluorescence) RBCs with FAM (green)-labeled iRGD-PEG (*Figure 2A*). Further confocal microscopy examination confirmed the effective conjugation of FAM (green)-labeled iRGD-PEG and DiI (red)-stained RBCs by yellow fluorescence observation (*Figure 2B,2C*). In addition, we performed an fluorescence intensity evaluation to determine the ligation efficacy of the iRGD to RBCs. According to

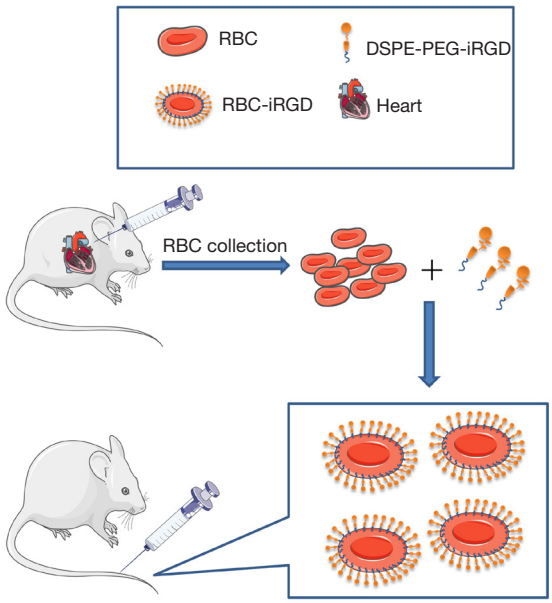

Figure 1 Schematic illustration to show the fabrication of RBC-iRGD and the therapeutic application in mice. RBC, red blood cell; DSPE, 1,2-distearoyl-sn-glycero-3-phosphoethanolamine-N-[succinyl(polyethylene glycol)-3400]; PEG, polyethylene glycol; iRGD, internalizing arginine-glycine-aspartic acid RGD.

the intensity and linear regression equation (*Figure 2D-2E*), an approximate 10^8 iRGD molecules were labeled on a single RBC.

Stability evaluation of the RBC-iRGD

After constructing the RBC-iRGD, we further examined their stability by comparing RBCs and RBC + iRGD. As shown in *Figure 3A*, the gross examination showed a similar appearance among RBC-iRGD, RBCs, and RBC + iRGD. We also incubated the RBC-iRGD, RBCs, and RBC + iRGD with RPMI 1640 medium containing 10% FBS for 48 h, and similar cell precipitates could be observed among RBC-iRGD, RBCs, and RBC + iRGD without hemolytic effects (*Figure 3B*). Further fluorescence decay evaluation showed a more than 80% fluorescence intensity after 48-h incubation, which was comparable to that of DiI stained RBCs (*Figure 3C-3F*).

Target efficacy of RBC-iRGD in subcutaneous gastric tumor mice

After completing the stability evaluation, a subcutaneous gastric tumor mouse model was established by injection of MKN-45 cells and subsequent target efficacy evaluation with RBC-iRGD. More effective tumor tracking illustrated by higher fluorescence intensity could be observed in RBC-iRGD compared to RBCs alone or RBC + iRGD in a 60-h period, which was evidenced by *in vivo* (*Figure 4A*) and *ex vitro* image (*Figure 4B*) and quantification (*Figure 4C*) data. Moreover, decreased liver and spleen accumulation could be found in RBC-iRGD-injected mice compared to RBC + iRGD-injected mice, whereas higher fluorescence accumulation could be observed in RBC-injected mice. In addition, the tumor section further confirmed the excellent target efficacy of RBC-iRGD (*Figure 4D-4F*).

RBC-iRGD exerted enhanced RT sensitivity effects in subcutaneous gastric tumor mice

After confirmation of the target efficacy of the RBC-iRGD, further evaluation on enhanced RT sensitivity effects with RBC-iRGD was performed. The procedure design is outlined in *Figure 5A*. Significantly decreased tumor volume could be observed in mice treated with RBC + iRGD plus RT compared to those treated with RBC alone and control mice. Moreover, the highest tumor volume decrease was observed in mice treated with RBC-iRGD and RT compared to those treated with RT only mice and RBC + iRGD and RT (*Figure 5B*). Moreover, RT or different modification on the RBCs did not affect the bodyweight of mice (*Figure 5C*). In addition, RT or additional modification of the RBCs did not affect the major organs (*Figure 5D*).

Discussion

The development of tumor-specific RT sensitizers is essential for radiation therapy. iRGD was initially used for tumor-specific delivery of small-molecule compounds (11). Previously, we found *in vivo* and *in vitro* experiments that free iRGD can increase the radiosensitivity of breast cancer cells 4T1 via remodeling tumor tissue penetration (17). However, free iRGD is quickly metabolized by the body's liver and spleen. RBCs are autologous and have good biocompatibility (20-22). Based on this, we speculated whether the combination of the iRGD and RBCs could offer both tumor targeting and biocompatibility and whether iRGD could be inserted into the surface of RBCs to improve its tumor targetability and further increase radiosensitivity. We were encouraged by our previous success in constructing iRGD-modified T cells and the proof that iRGD could also

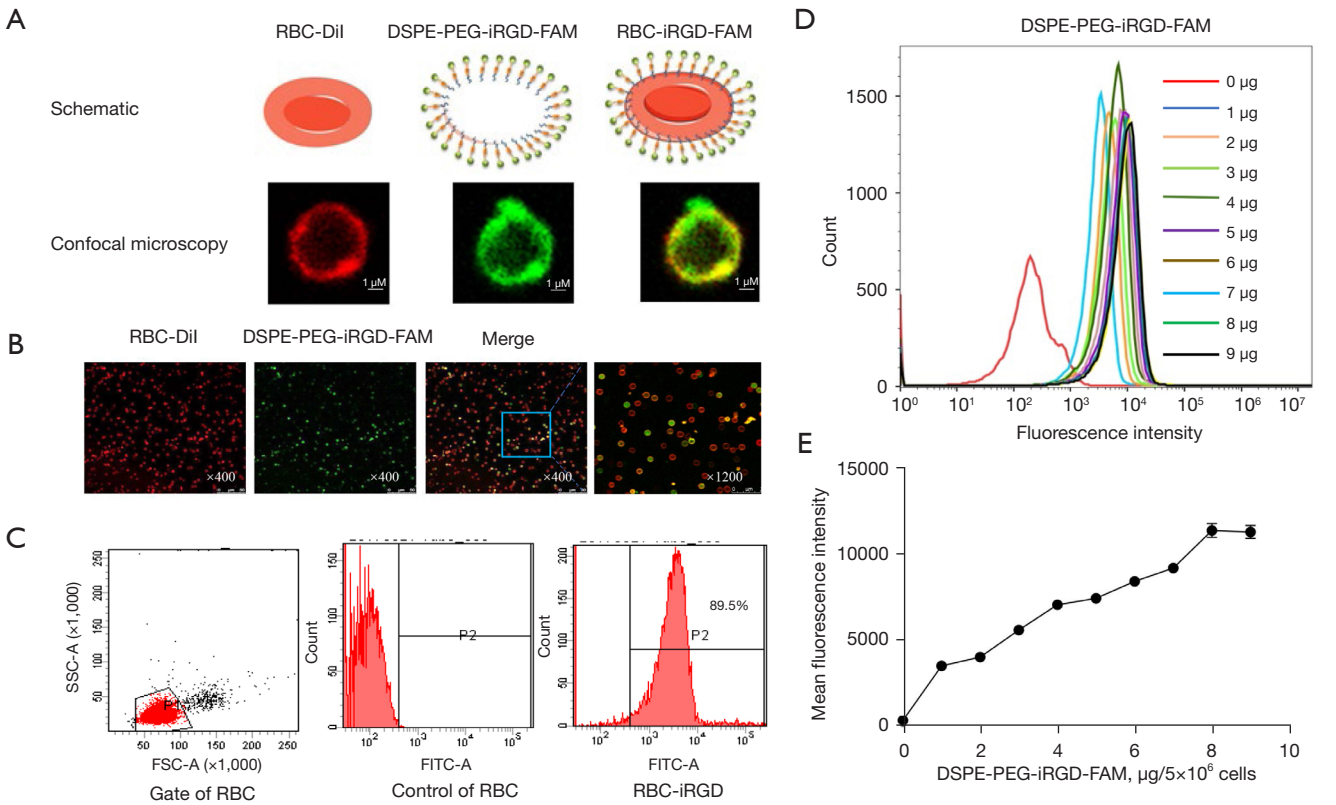

Figure 2 Fabrication of iRGD modified RBCs. (A) Upper layer, schematic illustration to show the fabrication of RBC-iRGD by modification of DiI (red)-stained RBCs with FAM (green)-labeled iRGD-PEG. Under layer, confocal microscopy images of single-channel red staining and green staining, and merged images of a single iRGD-modified RBC. Scale bar =1 μm. (B) Confocal microscopy images of single-channel red staining and green staining, and merged images of a iRGD-modified RBC population. Scale bar =50 μm. (C) Fluorescence-intensity evaluation of the RBC-iRGD. The figure on the left is the gate of control RBC. Flow cytometry histograms of RBCs alone (middle) and RBCs incubated with DSPE-PEG-iRGD-FAM (right). (D) Correlation analysis between the MFI and iRGD concentration (μg). Flow cytometry histograms of RBC incubated with different amounts of DSPE-PEG-iRGD-FAM. (E) Correlation analysis between the MFI and iRGD concentration (μg). Data are expressed with mean ± SD; n=3. RBC, Red blood cell; DiI, 1,1'-dioctadecyl-3,3,3',3'-tetramethylindocarbocyanine perchlorate; DSPE, 1,2-distearoyl-sn-glycero-3-phosphoethanolamine; PEG, polyethylene glycol; iRGD, arginylglycylaspartic acid; FAM, carboxyfluorescein; SSC-A, side scatter area; FSC-A, forward scatter area; FITC-A, fluorescein isothiocyanate; MFI, mean fluorescence intensity.

facilitate the infiltration of lymphocytes (16). In this study, we used the same liposome insertion technique to construct RBC-iRGD. Our study found first that connecting iRGD to the surface of RBC is not only more efficient, but also has high stability. Second, RBC-iRGD exerted good tumor-targeting efficacy. Third, RBC-iRGD could increase the sensitivity of radiation therapy for GC without causing severe side effects.

We used the lipid insertion to modify murine red blood cells with tumor-penetrating peptide iRGD. This method allows iRGD efficiently modify large numbers of RBCs without the need for complex procedures (19,22). We observed the morphology of RBC-iRGD by confocal microscopy and found no significant differences in the size and morphology between iRGD-mounted RBCs and ordinary RBCs.

In recent years, a considerable amount of research on the resistance and sensitization of tumor RT, chemotherapy, immunotherapy, and targeted therapy has emerged, especially in the field of nanomaterials and small biological molecules (23-26). In our team's previous work, we successfully constructed the recombinant protein iRGD-

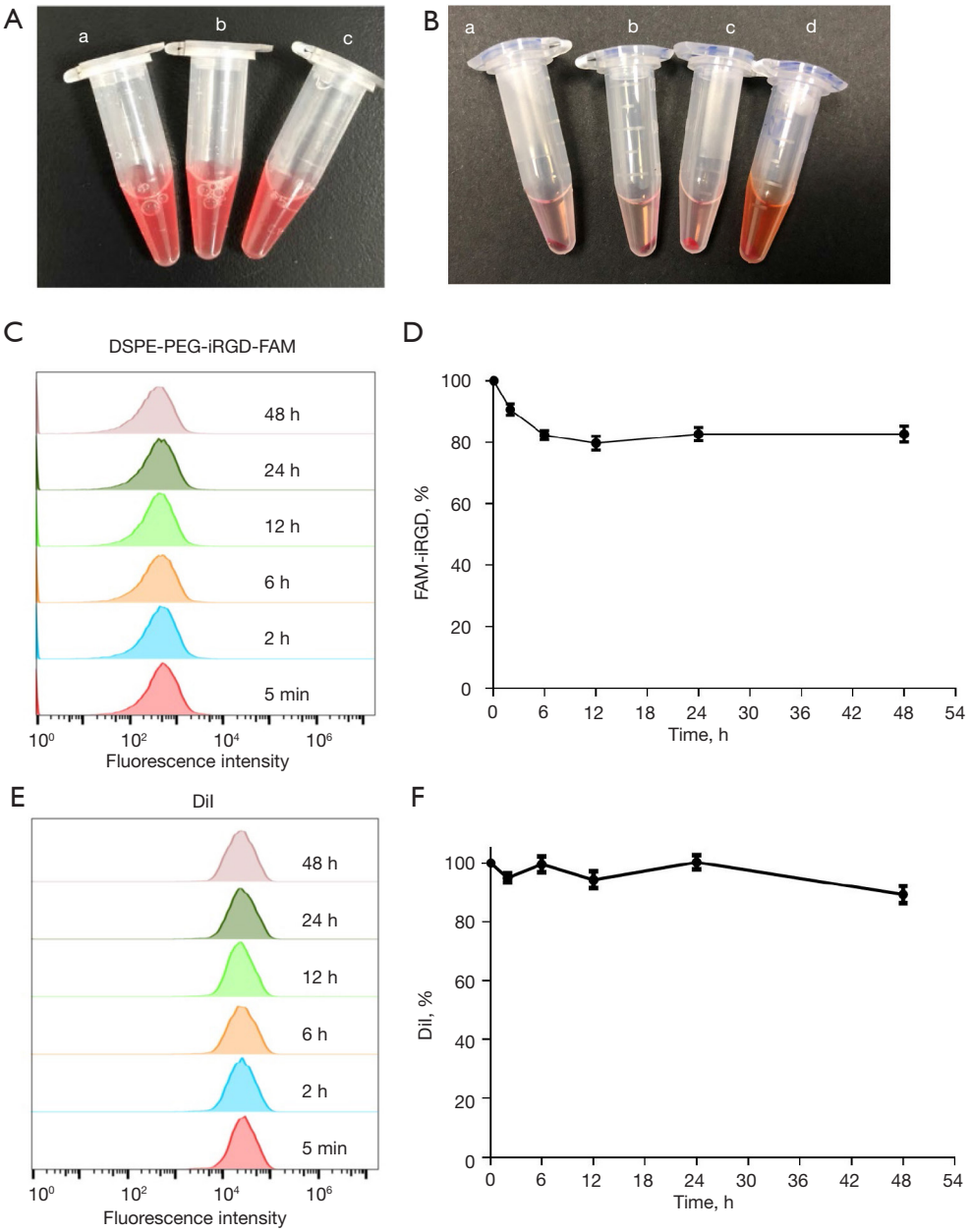

Figure 3 Stability evaluation of the RBC-iRGD. (A) Images of RBCs with different modifications: (a) RBC; (b) RBC + iRGD; (c) RBC-iRGD. (B) Images of RBCs with different modifications after storage in RPMI 1640 medium containing 10% fetal bovine serum for 48 h: (a) RBC; (b) RBC + iRGD; (c) RBC-iRGD; (d) hemolytic RBCs. (C) FAM fluorescence evaluation of the RBC-iRGD at different time points. (D) Analysis of the percentage of FAM-iRGD using flow cytometry. (E) DiI fluorescence evaluation of the DiI stained RBCs at different time points. (F) Analysis of the percentage of DiI stained RBCs using flow cytometry. DSPE, 1,2-distearoyl-sn-glycero-3-phosphoethanolamine; PEG, polyethylene glycol; iRGD, internalizing arginine-glycine-aspartic acid RGD; FAM, carboxyfluorescein; DiI,1,1'-dioctadecyl-3,3,3',3'-tetramethylindocarbocyanine perchlorate; RBC, red blood cell.

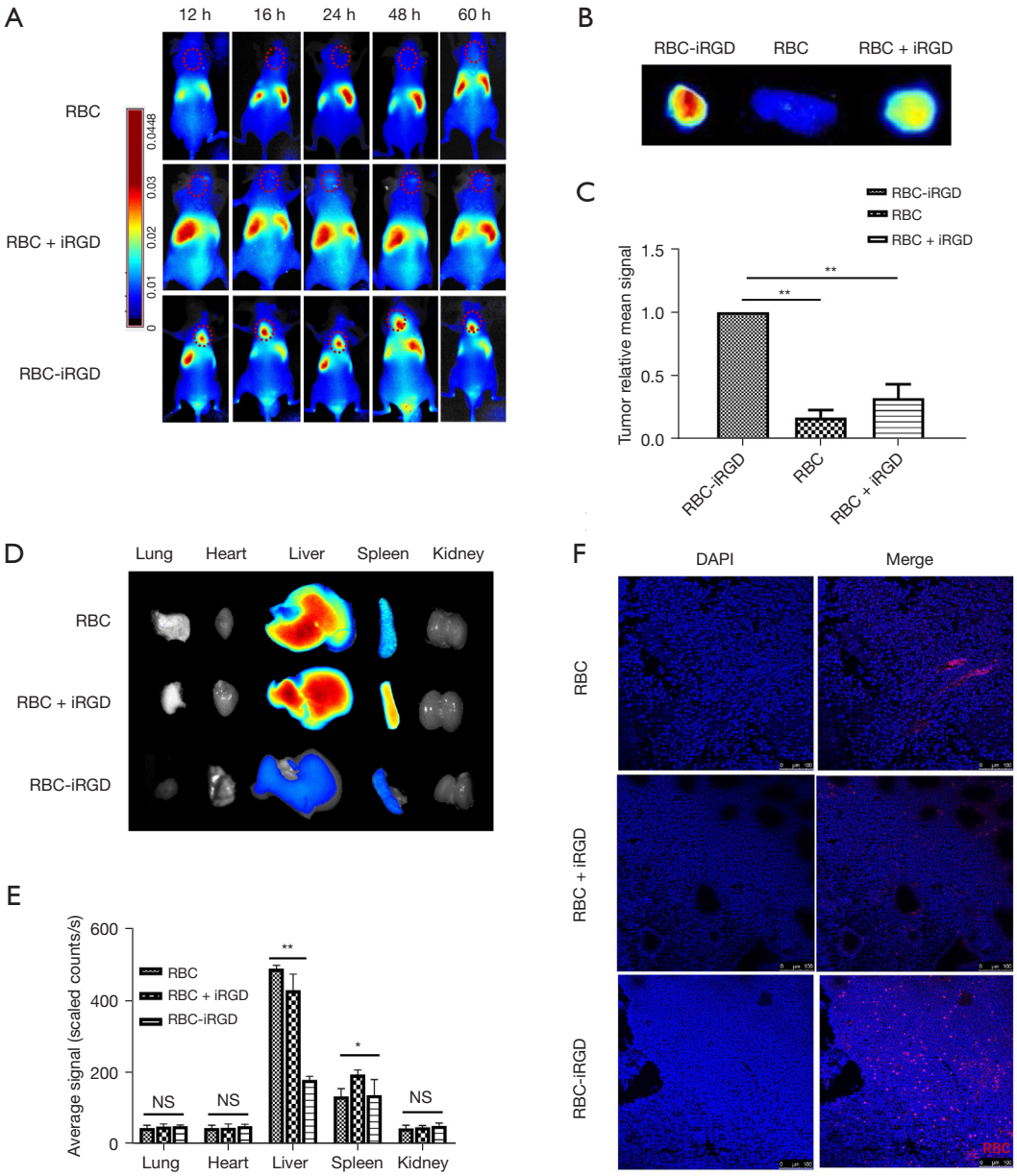

Figure 4 Tumor targeting ability of iRGD modified RBCs in a systematic administration route. (A) A tumor-bearing nude mice was established by subcutaneous injection of MKN-45 cells, followed by DiR stained RBCs, RBC + iRGD, and RBC-iRGD injection for tumor tracking. Effective tumor tracking could be observed in mice treated with RBC-iRGD compared to those treated with RBCs alone or RBC + iRGD in a 60-h period. Red dashed lines, subcutaneous tumors. (B) Fluorescence intensity evaluation on incised tumors from mice injected with RBCs, RBC + iRGD, and RBC-iRGD. Apparent fluorescence accumulation could be observed tumors treated with RBC-iRGD compared to those treated with RBCs alone or RBC + iRGD. (C) A significantly decreased fluorescence signal could be observed in tumor tissues from mice injected with RBCs alone or RBC + iRGD compared to those injected with RBC-iRGD. (D) Organ fluorescence intensity evaluation for the safety purpose. Less accumulated fluorescence intensity could be observed in the liver and spleen from RBC-iRGD injected mice compared to those with RBC + iRGD. (E) Organ fluorescence intensity evaluation of safety. Less accumulation of fluorescence intensity could be observed in the liver and spleen from RBC-iRGD–injected mice compared to those treated with RBC + iRGD. (F) Fluorescence signaling distribution analysis of the tumor sections from mice injected with RBCs, RBC + iRGD and RBC-iRGD. *, P<0.05; **, P<0.01; NS, not significant. RBC, red blood cell; iRGD, internalizing arginine-glycine-aspartic acid RGD; DAPI, 4',6-diamidino-2-phenylindole.

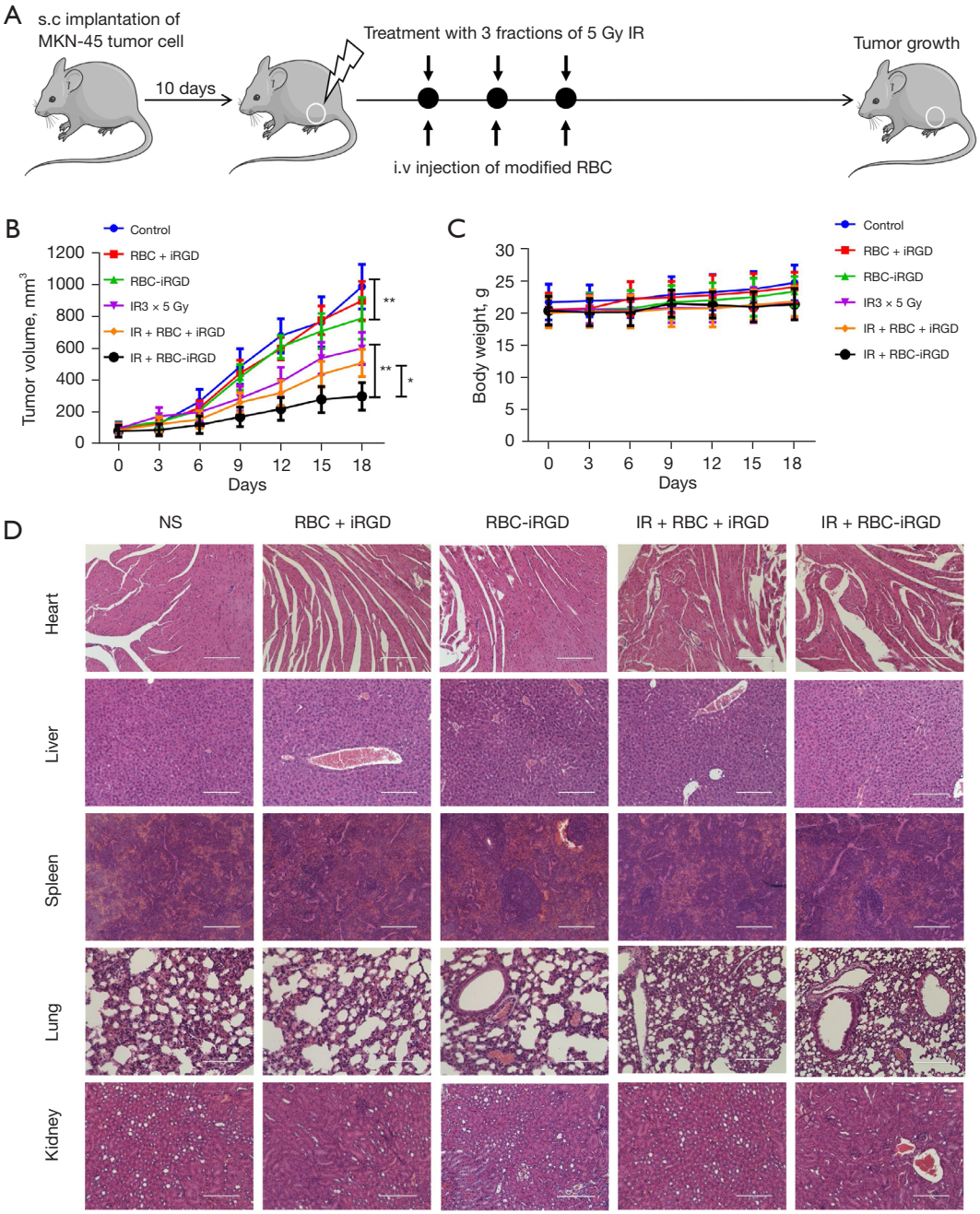

Figure 5 Efficacy of RBC-iRGD in enhancement of radiotherapy in subcutaneous gastric tumor mice. (A) Schematic illustration shows the generation of the subcutaneous gastric tumor mice model, treatment with radiotherapy (5 Gy radiotherapy, 3 fractions), and RBC + iRGD and RBC-iRGD injection to monitor the tumor growth. (B) Tumor volume monitoring. A significantly decreased tumor volume could be observed in mice treated with RBC + iRGD plus radiotherapy compared to those treated with RBCs alone and control mice. Moreover, the highest tumor volume decrease was observed in mice treated with RBC-iRGD plus radiotherapy compared to those treated with radiotherapy alone and RBC + iRGD plus radiotherapy. **, P<0.01; *, P<0.05. (C) Radiotherapy or different modification on the RBCs had no effect on the bodyweight of mice. (D) HE-stained sections of major organs including the heart, liver, spleen, lungs, and kidneys collected from mice with different treatments on Day 18. Scale bar =200 μm. Radiotherapy or different modification on the RBCs did not affect the major organs. RBC, red blood cell; iRGD, internalizing arginine-glycine-aspartic acid RGD; HE, hematoxylin and eosin; IR, irradiation.

antiCD3 and demonstrated its antitumor efficacy by promoting T cell activation and infiltration. We also found that combining iRGD-antiCD3 with PD-1 blocking can further improve the anti-tumor efficacy of T cells (27).

There are some limitations in this study that could be addressed in future research. The molecular mechanisms of enhancement the sensitivity of radiation therapy have not been explored in depth. Whether the RBC-iRGD with loading drugs can further improve the efficacy. In our future work, we will combine iRGD with drug-carrying or tumor-specific-antigens-carrying erythrocytes to try to further improve the effect of immunotherapy of tumors.

In summary, we designed and fabricated RBC-iRGD for tumor targeting and therapy enhancement. We subsequently followed this with an evaluation of its safety and efficacy *in vivo* and explored the possible mechanisms involved in its effects using *in vitro* cell system. The results demonstrated that RBC-iRGD exerted good tumor targeting efficacy and favorable effects for RT enhancement *in vivo*.

Acknowledgments

Funding: This work was supported by the National Natural Science Foundation of China (No. 82072926) and the Youth Medical Science and Technology Innovation Project of Xuzhou Health Committee (No. XWKYHT20200024).

Footnote

Reporting Checklist: The authors have completed the ARRIVE reporting checklist. Available at https://jgo.amegroups.com/article/view/10.21037/jgo-22-951/rc

Data Sharing Statement: Available at https://jgo.amegroups.com/article/view/10.21037/jgo-22-951/dss

Conflicts of Interest: All authors have completed the ICMJE uniform disclosure form (available at https://jgo.amegroups.com/article/view/10.21037/jgo-22-951/coif). The authors have no conflicts of interest to declare.

Ethical Statement: The authors are accountable for all aspects of the work in ensuring that questions related to the accuracy or integrity of any part of the work are appropriately investigated and resolved. Experiments were performed under a project license (No. 20150902) granted by the Animal Care Committee at Nanjing Drum Tower Hospital, in compliance with Nanjing Drum Tower Hospital guidelines for the care and use of animals.

References

1. Thrift AP, El-Serag HB. Burden of Gastric Cancer. Clin Gastroenterol Hepatol 2020;18:534-42.
2. Wei J, Wu ND, Liu BR. Regional but fatal: Intraperitoneal metastasis in gastric cancer. World J Gastroenterol 2016;22:7478-85.
3. Foo M, Crosby T, Rackley T, et al. Role of (chemo)-radiotherapy in resectable gastric cancer. Clin Oncol (R Coll Radiol) 2014;26:541-50.
4. Lee J, Byun HK, Koom WS, et al. Efficacy of radiotherapy for gastric bleeding associated with advanced gastric cancer. Radiat Oncol 2021;16:161.
5. Lordick F, Nilsson M, Leong T. Adjuvant radiotherapy for gastric cancer-end of the road? Ann Oncol 2021;32:287-9.
6. Glinski K, Wasilewska-Tesluk E, Rucinska M, et al. Clinical outcome and toxicity of 3D-conformal radiotherapy combined with chemotherapy based on the Intergroup SWOG 9008/INT0116 study protocol for gastric cancer. J BUON 2015;20:428-37.
7. Kassam Z, Mackay H, Buckley CA, et al. Evaluating the impact on quality of life of chemoradiation in gastric cancer. Curr Oncol 2010;17:77-84.
8. Zhang H, Barralet JE. Mimicking oxygen delivery and waste removal functions of blood. Adv Drug Deliv Rev 2017;122:84-104.
9. Gao C, Lin Z, Wang D, et al. Red Blood Cell-Mimicking Micromotor for Active Photodynamic Cancer Therapy. ACS Appl Mater Interfaces 2019;11:23392-400.
10. Fang H, Gai Y, Wang S, et al. Biomimetic oxygen delivery nanoparticles for enhancing photodynamic therapy in triple-negative breast cancer. J Nanobiotechnology 2021;19:81.
11. Kang S, Lee S, Park S. iRGD Peptide as a Tumor-Penetrating Enhancer for Tumor-Targeted Drug Delivery. Polymers (Basel) 2020;12:1906.

12. Chen H, Sha H, Zhang L, et al. Lipid insertion enables targeted functionalization of paclitaxel-loaded erythrocyte membrane nanosystem by tumor-penetrating bispecific recombinant protein. Int J Nanomedicine 2018;13:5347-59.
13. Huang Y, Li X, Sha H, et al. Tumor-penetrating peptide fused to a pro-apoptotic peptide facilitates effective gastric cancer therapy. Oncol Rep 2017;37:2063-70.
14. Zhu A, Sha H, Su S, et al. Bispecific tumor-penetrating protein anti-EGFR-iRGD efficiently enhances the infiltration of lymphocytes in gastric cancer. Am J Cancer Res 2018;8:91-105.
15. Dean A, Gill S, McGregor M, et al. Dual αV-integrin and neuropilin-1 targeting peptide CEND-1 plus nab-paclitaxel and gemcitabine for the treatment of metastatic pancreatic ductal adenocarcinoma: a first-in-human, open-label, multicentre, phase 1 study. Lancet Gastroenterol Hepatol 2022;7:943-51.
16. Ding N, Zou Z, Sha H, et al. iRGD synergizes with PD-1 knockout immunotherapy by enhancing lymphocyte infiltration in gastric cancer. Nat Commun 2019;10:1336.
17. Meng F, Liu J, Wei J, et al. Tumor-penetrating peptide internalizing RGD enhances radiotherapy efficacy through reducing tumor hypoxia. Cancer Sci 2022;113:1417-27.
18. Fang RH, Hu CM, Chen KN, et al. Lipid-insertion enables targeting functionalization of erythrocyte membrane-cloaked nanoparticles. Nanoscale 2013;5:8884-8.
19. Shi G, Mukthavaram R, Kesari S, et al. Distearoyl anchor-painted erythrocytes with prolonged ligand retention and circulation properties in vivo. Adv Healthc Mater 2014;3:142-8.
20. Chu Y, Zhang J, Pan H, et al. Preparation and evaluation of long circulating erythrocyte membrane-cloaked anti-cancer drug delivery system. Drug Deliv Transl Res 2020;10:1278-87.
21. Daniyal M, Jian Y, Xiao F, et al. Development of a nanodrug-delivery system camouflaged by erythrocyte membranes for the chemo/phototherapy of cancer. Nanomedicine (Lond) 2020;15:691-709.
22. Mukthavaram R, Shi G, Kesari S, et al. Targeting and depletion of circulating leukocytes and cancer cells by lipophilic antibody-modified erythrocytes. J Control Release 2014;183:146-53.
23. Abed S, Turner R, Serniuck N, et al. Cell-specific drug targeting in the lung. Biochem Pharmacol 2021;190:114577.
24. Dong Z, Wang C, Gong Y, et al. Chemical Modulation of Glucose Metabolism with a Fluorinated CaCO3 Nanoregulator Can Potentiate Radiotherapy by Programming Antitumor Immunity. ACS Nano 2022;16:13884-99.
25. Thangam R, Patel KD, Kang H, et al. Advances in Engineered Polymer Nanoparticle Tracking Platforms towards Cancer Immunotherapy-Current Status and Future Perspectives. Vaccines (Basel) 2021;9:935.
26. Yu Z, Lan J, Li W, et al. Circular RNA hsa_circ_0002360 Promotes Proliferation and Invasion and Inhibits Oxidative Stress in Gastric Cancer by Sponging miR-629-3p and Regulating the PDLIM4 Expression. Oxid Med Cell Longev 2022;2022:2775433.
27. Zhou S, Meng F, Du S, et al. Bifunctional iRGD-anti-CD3 enhances antitumor potency of T cells by facilitating tumor infiltration and T-cell activation. J Immunother Cancer 2021;9:e001925.

Cite this article as: Zhou C, Liu Q, Meng F, Ding N, Yan J, Liu B. Modification of erythrocytes by internalizing Arg-Gly-Asp (iRGD) in boosting the curative effect of radiotherapy for gastric carcinoma. J Gastrointest Oncol 2022;13(5):2249-2258. doi: 10.21037/jgo-22-951

